Check for updates

Received: 10 May 2023 | Revised: 15 July 2023 | Accepted: 22 July 2023

DOI: 10.1111/pce.14676

ORIGINAL ARTICLE

Plant, Cell & Environment | WILEY

Abscisic acid acts essentially on stomata, not on the xylem, to improve drought resistance in tomato

Eduardo J. Haverroth[1,2] | Leonardo A. Oliveira[1,2] | Moab T. Andrade[2] | Matthew Taggart[1] | Scott A. M. McAdam[3] | Agustin Zsögön[2] | Andrew J. Thompson[4] | Samuel C. V. Martins[2] | Amanda A. Cardoso[1]

[1]Department of Crop and Soil Sciences, North Carolina State University, Raleigh, North Carolina, USA

[2]Departamento de Biologia Vegetal, Universidade Federal de Viçosa, Viçosa, Minas Gerais, Brazil

[3]Department of Botany and Plant Pathology, Purdue University, West Lafayette, Indiana, USA

[4]Centre for Soil, Agrifood and Biosciences, Cranfield University, Bedfordshire, UK

Correspondence

Samuel C. V. Martins, Departamento de Biologia Vegetal, Universidade Federal de Viçosa, Viçosa, MG 36570-900, Brazil.
Email: samuel.martins@ufv.br

Amanda A. Cardoso, Department of Crop and Soil Sciences, North Carolina State University, Raleigh, NC 27695, USA.
Email: aavilac@ncsu.edu

Funding information

U.S. Department of Agriculture; National Science Foundation, Grant/Award Number: IOS-2140119

Abstract

Drought resistance is essential for plant production under water-limiting environments. Abscisic acid (ABA) plays a critical role in stomata but its impact on hydraulic function beyond the stomata is far less studied. We selected genotypes differing in their ability to accumulate ABA to investigate its role in drought-induced dysfunction. All genotypes exhibited similar leaf and stem embolism resistance regardless of differences in ABA levels. Their leaf hydraulic resistance was also similar. Differences were only observed between the two extreme genotypes: *sitiens* (*sit*; a strong ABA-deficient mutant) and *sp12* (a transgenic line that constitutively overaccumulates ABA), where the water potential inducing 50% embolism was 0.25 MPa lower in *sp12* than in *sit*. Maximum stomatal and minimum leaf conductances were considerably lower in plants with higher ABA (wild type [WT] and *sp12*) than in ABA-deficient mutants. Variations in gas exchange across genotypes were associated with ABA levels and differences in stomatal density and size. The lower water loss in plants with higher ABA meant that lethal water potentials associated with embolism occurred later during drought in *sp12* plants, followed by WT, and then by the ABA-deficient mutants. Therefore, the primary pathway by which ABA enhances drought resistance is via declines in water loss, which delays dehydration and hydraulic dysfunction.

KEYWORDS

embolism resistance, hydraulic vulnerability, minimum leaf conductance, *Solanum lycopersicum*, water deficit, water loss

1 | INTRODUCTION

Soil drought has been the most detrimental abiotic stress threatening crop production since agricultural emergence in the Neolithic period (Lesk et al., 2016). With ongoing climate changes, even more frequent and severe droughts are predicted to occur in the coming decades, challenging food production in the face of an ever-increasing population (Dai, 2013; Lesk et al., 2016; Lobell & Field, 2007). Soil drought impacts different plant processes depending on the level of tissue dehydration. Declines in water content first

This is an open access article under the terms of the Creative Commons Attribution License, which permits use, distribution and reproduction in any medium, provided the original work is properly cited.
© 2023 The Authors. *Plant, Cell & Environment* published by John Wiley & Sons Ltd.

impair cellular expansion and close stomata limiting CO_2 uptake; then further plant dehydration can lead to extensive damage to the water transport system and ultimately, plant death (Scoffoni et al., 2017; Trueba et al., 2019; Tyree & Sperry, 1989).

For plants to grow and produce, water must be absorbed from the soil by the roots and then transported within the plant through the xylem until it reaches the stomata on the leaf surface. Once in the leaves, water vapor is lost through transpiration (*E*) as the stomata open to allow the acquisition of CO_2 for photosynthesis (*A*). The ascent of movement of water within the xylem of plants is explained by the 'cohesion-tension' theory (Dixon & Joly, 1895), where water moves under tension driven by a gradient of water potential (Venturas et al., 2017). During drought, the risk of xylem dysfunction by embolism increases as the tension in the xylem intensifies (Tyree & Sperry, 1989). Cavitation occurs when the xylem tension reaches a threshold at which tiny air bubbles are pulled into the xylem cells. When inside the xylem, the xylem tension causes these bubbles to rapidly expand, blocking the water transport in that specific xylem conduit (i.e., embolism) (Tyree & Sperry, 1989).

Embolism negatively impacts whole-plant function given the declines in the water transport efficiency (hydraulic conductance, *K*) that occur when it forms. Consequently, plants that have evolved xylem highly resistant to embolism are likely more tolerant to low water potentials and drought (McAdam and Cardoso, 2019). Xylem resistance to embolism has been shown to vary enormously across (Choat et al., 2012) and within species (Cardoso et al., 2020, 2022; Johnson et al., 2022; Rodriguez-Dominguez et al., 2018). Species with narrower xylem vessels are often more resistant to embolism than species with wider conduits (Isasa et al., 2023). Similarly, a higher xylem cell wall thickness to lumen breadth ratio has been correlated with a higher embolism resistance (Blackman et al., 2010; Cardoso et al., 2018), as well as thicker pit membranes (Dória et al., 2018; Thonglim et al., 2023, 2021) and a minimally connected xylem network (Avila et al., 2023; Loepfe et al., 2007; Mrad et al., 2021).

Another mechanism allowing seed plants to minimize tissue dehydration and xylem embolism during drought is the accumulation of foliar abscisic acid (ABA) and consequent stomatal closure (Daszkowska-Golec & Szarejko, 2013). As water potential declines during drought, so does the turgor (Creelman & Zeevaart, 1985; Pierce & Raschke, 1980) and volume of leaf cells, triggering the accumulation of ABA primarily in leaves (McAdam & Brodribb, 2016; Zhang et al., 2018). In leaves, the mesophyll is the primary source of drought-induced accumulation of ABA (McAdam & Brodribb, 2018). ABA triggers stomata closure by activating anion channels in the guard cell membrane, actively lowering guard cell turgor (Daszkowska-Golec & Szarejko, 2013). The declines in stomatal conductance (g_s) driven by ABA delay the drought-induced plant dehydration and embolism formation, maintaining plants at a safer water potential range (Cardoso et al., 2018; Creek et al., 2020). ABA also (i) improves water-use efficiency (WUE) by lowering g_s while maintaining *A*, (ii) enhances root growth and root hydraulic conductance, and (iii) allows plants to sustain growth during drought (Mega et al., 2019; Thompson, Andrews, et al., 2007). The prominent role of ABA in plant function during drought has triggered numerous studies focused on manipulating ABA levels or signal transduction by both chemical (Helander et al., 2016) and transgenic approaches (Thompson, Andrews, et al., 2007) aiming at improving WUE and drought resistance in crops.

Recent work has presented evidence that appears to quell hopes for enhancing drought resistance in crops through manipulated increases in ABA levels (Lamarque et al., 2020). Lamarque et al. (2020) found that a transgenic line of tomato (*Solanum lycopersicum* L.) that constitutively overaccumulates ABA (*sp12*) exhibits lower (from c. 0.5 to 1.2 MPa) stem xylem resistance to embolism than the wild type (WT). In the absence of a drought experiment, however, we are unsure of whether this transgenic ABA line with a less resistant xylem is, in fact, less drought resistant. It is possible that plants overaccumulating ABA exhibit such a conservative mechanism in terms of low water loss, that during drought, plant dehydration is considerably delayed, and plant survival is further prolonged, rendering these plants more drought tolerant than their WT, despite the less resistant xylem to embolism.

In this study, we aimed to better understand the role of ABA in promoting drought resistance through such opposing mechanisms in the xylem and the stomata. We also assessed, for the first time, the impact of ABA on the minimum leaf conductance (g_{min})—the leaf conductance to water vapor through the cuticle and incompletely closed stomata) (Duursma et al., 2019). To address these gaps, we selected four tomato lines differing in the ability to accumulate ABA. The WT cv. Ailsa Craig. Two near-isogenic lines carrying mutations in ABA biosynthesis genes: *sitiens* (*sit*)—deficient in ABA-aldehyde oxidase (Harrison et al., 2011)—and *notabilis* (*not*)—deficient in the rate-limiting enzyme of ABA biosynthesis, 9-*cis*-epoxycarotenoid dioxygenase (NCED) (Burbidge et al., 1999). And finally, a transgenic line in the Ailsa Craig genetic background (*sp12*) overexpressing NCED from a constitutive promoter, and thus overaccumulating ABA (Thompson, Andrews, et al., 2007; Thompson, Jackson, et al., 2000; Thompson, Mulholland, et al., 2007). We hypothesized that, despite potential increases in stem xylem resistance to embolism, the primary role of ABA in regulating drought resistance is via stomatal regulation. Plants overaccumulating ABA would be able to delay declines in water potential below the threshold for which embolism and hydraulic dysfunction occur, thus conferring higher drought resistance to this genotype.

2 | MATERIALS AND METHODS

2.1 | Plant material

Seeds of WT, *sit* and *not* were provided by Agustin Zsögön (Universidade Federal de Vicosa, Brazil), and seeds of *sp12* were provided by A. Thompson (Cranfield University, UK). Seeds were first germinated in a mixture of 50% Sun Gro Propagation Growing Mix and 50% sand. Germination was considered when both cotyledons

had fully emerged, which occurred after c. 20 days for *sp12* and c. 5 days for *sit*, *not* and WT. Because of the difference in germination time, plants of *sp12* were sowed 15 days before the sowing of *sit*, *not* and WT seeds. Therefore, plants were at the same age for all experiments.

One-week seedlings were individually transplanted into 6-L plastic pots containing the substrate aforementioned. Plants were cultivated in an environmentally controlled chamber. Conditions in the chambers were set to 0600:1800 photoperiod with photosynthetic photon flux density (PPFD) of c. 600 µmol m^{-2} s^{-1}, day:-night temperature cycles of 26:22°C, and ambient levels of CO_2 (c. 420 µmol mol^{-1}). Relative humidity in the chamber was not controlled and ranged from 50% to 70%. Daily irrigation with nutrient solution (Supporting Information: Table S1) was performed to field capacity until plants achieved 60 days old. Plant age was calculated from the day of emergence. For the following methods, samplings were performed such that less than 20% of the total leaf area of the plants was cut.

2.1.1 | Quantification of ABA

The ABA was quantified from healthy and fully expanded leaves from the middle third of the plant shoot ($n = 6$). Sampling was performed in well-watered plants as a means to confirm differences in the intrinsic ability to accumulate ABA across the four genotypes. Samples were weighed, covered in cold (−30°C) 80% (v/v) methanol in water, and immediately stored at −20°C. They were further purified, and the foliar ABA level was quantified by physicochemical methods with an added internal standard using an Agilent 6400 series triple quadrupole liquid chromatography/mass spectrometry (Agilent) according to McAdam (2015). Foliar ABA levels were expressed in terms of dry weight (DW), which was quantified after ABA determination by weighing the dry mass of the sample harvested and extracted for analysis. Normalizing the ABA levels to tissue DW avoids passive increases in ABA levels as cells dehydrate.

2.2 | Optical vulnerability curves

The vulnerability curves of leaves and stems were assessed through the optical vulnerability method (Brodribb et al., 2016). Six plants from each genotype ($n = 6$) were brought to the laboratory during the evening, removed from the pots, and had their roots carefully washed. They were maintained overnight with their roots underwater with aeration systems to ensure that roots would not suffer from hypoxia. During the next morning, one leaf per plant (the youngest fully expanded leaf) was set up on a microscope (LCD digital microscope; New York Microscope Company) adapted with a bottom light source, while remaining attached to the plant. The leaf was fixed under the microscope using transparent adhesive. From the same plant, we also attached a middle portion of the stem to another microscope. For the stem, the xylem was exposed carefully using a razor blade and then covered with conductive adhesive gel (Parker Labs) and a cover slip. Images from leaves and stems were taken every 180 s as the plant dehydrated under dark conditions (to induce water potential equilibration throughout the plant), with their roots exposed to air to accelerate plant dehydration. The plant water potential (Ψ_w) was periodically measured using a stem psychrometer (ICT). Leaf water potentials were also measured over time using a pressure chamber to confirm the measurements obtained from the psychrometer. Embolisms were determined by a visible change in colour in xylem conduits. The area of embolism was quantified by image subtraction of stacks of images using ImageJ software (National Institutes of Health). Complete descriptive details of this method are available on the open-source website http://www.opensourceov.org. To analyze the relationship between plant water potential and embolism formation, a linear regression was fitted between time and Ψ_w, so the Ψ_w of each image could be determined. Mean and standard errors for vulnerability curves were determined for every 1% of the embolized xylem area and plotted as per (Cardoso et al., 2022). The Ψ_w at 12%, 50%, and 88% cumulative embolism (P_{12}, P_{50} and P_{88}) were obtained for each curve.

2.3 | Leaf hydraulic vulnerability curves

Leaf hydraulic vulnerability curves describing the declines in leaf hydraulic conductance (K_{leaf}) with dehydration were constructed using the dynamic rehydration kinetics method (Blackman & Brodribb, 2011; Brodribb & Cochard, 2009). Only fully expanded leaves from the middle third of the plant shoot were utilized. Maximum K_{leaf} was determined from a subset of six well-watered plants ($n = 6$). Then, plants were allowed to dehydrate due to irrigation withholding and K_{leaf} was determined sequentially by measuring the rehydration flux of water using a hydraulic flowmeter. Before each measurement, a leaf was sampled to determine the minimum leaf water potential (Ψ_{leaf}) to construct the hydraulic curve. Ψ_{leaf} were assessed using a Scholander chamber (Model 1505D; PMS Instruments). Then, a neighbouring leaf was excised underwater and immediately connected to the flowmeter, where the hydraulic flux into the leaf was logged every 3 s for 60 s or until the flow rate decayed. Subsequently, the leaf was disconnected, bagged, and left to equilibrate for 15 min to measure the final Ψ_{leaf} and leaf area. The initial and final instantaneous K_{leaf} were calculated from the following equation:

$$K_{leaf} = F/(\text{Leaf Area} \times \Delta\Psi_w),$$

where F is the instantaneous flow rate into the leaf (F, mmol m^{-2} s^{-1}) and $\Delta\Psi_w$ is the water potential gradient driving the flow, which is equal to final Ψ_{leaf}. Initial and final K_{leaf} were discarded when variation exceeded c. 30%. K_{leaf} values were normalized to 25°C. The relationship between K_{leaf} and initial Ψ_{leaf} was fitted by a three-parameter sigmoidal equation and used to construct the hydraulic vulnerability curve. From each curve, water potentials at 12%, 50%, and 88% of loss in K_{leaf} (P_{12}, P_{50} and P_{88}) were determined.

2.4 | Pressure–volume curves and minimum leaf hydraulic conductance

Pressure–volume curves (Tyree & Hammel, 1972) were performed using fully expanded, healthy leaves ($n = 6$). Leaves were sampled and rehydrated overnight to achieve Ψ_{leaf} c. −0.1 MPa. Then, they were allowed to dehydrate on a bench, while mass and Ψ_{leaf} were periodically measured using a digital balance (0.0001 g) and a Scholander chamber. Finally, leaves were placed in an oven at 70°C for at least 48 h to determine the dry mass. Leaf DW was used to calculate relative water content, which was plotted against $1/\Psi_{leaf}$. Ψ_{TLP} was estimated as the inflection point of the curve.

The g_{min} was measured according to the mass loss of water from the detached leaves method (Duursma et al., 2019). Fully expanded leaves ($n = 12$) were sampled at pre-dawn and had their petioles covered with parafilm. Next, leaves were scanned for leaf area and weighed immediately using a digital balance to four decimal places. Leaves were then suspended in a growth chamber, allowing slow desiccation. Measurements of leaf mass, temperature, and relative humidity were recorded every 30 min. After reaching water loss stability, leaves were dried at 70°C for at least 48 h and weighed to obtain leaf dry mass. The g_{min} was calculated from the slope of the latter linear region of the relationship between decreasing leaf mass (g) and increasing time (min). This was converted from $g^{-1}\,min^{-1}$ to $mmol\,m^{-2}\,s^{-1}$ by dividing by projected leaf area (m^2) and the mean chamber vapour pressure deficit (VPD), and converting the mass loss from g to mmol H_2O.

2.5 | Leaf anatomical traits

Leaf anatomical traits were assessed from healthy and fully expanded leaves ($n = 6$) from the middle third of the plant shoot. The following traits were estimated: stomatal density (D_s), stomatal length (L_s), and vein density (D_v). Stomatal measurements were performed on both epidermal sides. Leaves were cleared in 100% methanol for 48 h, followed by incubation in 95% lactic acid at 90°C until clarification. For each sample, 10 fields of view were imaged at either ×4 or ×20 magnification using a digital camera (Zeiss AxioCam HRc) mounted on a light microscope (AX70 TRF; Olympus Optical). Measurements were performed using Image-Pro Plus 4.5 (Media Cybernetics).

Hand-cut transverse sections from fresh stems of 60-day-old plants were also performed. The sections were stained for 5 min with a solution containing phloroglucinol–HCl (1:2) (2% [w:v] phloroglucinol in 95% alcohol and 5 M hydrochloric acid). Sections were stained with phloroglucinol so that the xylem area could be easily recognized. Images were taken using a digital camera (DP28; Olympus Optical) mounted on a stereo microscope (ZMS800; Nikon).

2.6 | Dry-down experiments

Once the embolism resistances of the genotypes were characterized, dry-down experiments were performed to assess whether the different genotypes would differ in terms of the time taken for plants to reach hydraulic dysfunction during drought (considered here as the mean stem P_{50} of the four genotypes, i.e., −1.30 MPa). In the afternoon before the experiment, a subset of four 60-day-old plants ($n = 4$) were watered until the full substrate capacity. The next day, irrigation was withheld from droughted plants until plants achieved Ψ_w of c. −1.30 MPa, where after plants were irrigated and maintained under well-watered conditions for two additional days. Leaf gas exchange and minimum Ψ_w (measured at midday) were measured daily during the entire experiment. Sampling did not affect more than 20% of the total leaf area per plant. Leaf gas exchange was measured using a Li-6800 (LI-COR; Lincoln) and conditions in the cuvette adjusted accordingly to the growth chamber conditions (PPFD of 600 $\mu mol\,m^{-2}\,s^{-1}$, 10% of blue light, VPD of 1.5 kPa, and CO_2 at 420 $\mu mol\,mol^{-1}$). The Ψ_w was measured in leaves using a Scholander chamber. On the second day after rewatering, the K_{leaf} was assessed using the evaporative flux method (Brodribb & Holbrook, 2006). For this experiment, the evaporative flux method was selected over the dynamic rehydration kinetics method as leaves had to be sampled and transported from the growth chamber to the laboratory underwater. One leaf per plant was collected underwater, transported as such to the laboratory and attached to a flowmeter. They were then placed under a PPFD of 1000 $\mu mol\,m^{-2}\,s^{-1}$ and had the water flow rate logged until flow reached stabilization. Leaves were then allowed to equilibrate for 15 min and had the Ψ_{leaf} measured using a Scholander chamber. The K_{leaf} was calculated from the following equation:

$$K_{leaf} = F \times V_{leaf}/(-\Psi_{leaf}),$$

where K_{leaf} = leaf hydraulic conductance ($mmol\,m^{-2}\,s^{-1}\,MPa^{-1}$); V_{leaf} = viscosity of water in the sample leaf relative to 25°C; and Ψ_{leaf} in MPa. K_{leaf} was normalized by leaf area.

Because of changes in plant morphology (plant height, internode length and leaf rachis length) across the adult plants of the four genotypes, another dry-down experiment was performed using 20-day-old seedlings ($n = 4$). These seedlings were young enough to not display changes in plant height and internode length, such that only total leaf area, g_s, and g_{min} would affect the water loss rate and the time for wilting and death. Seedlings were watered to pot capacity and excess water was allowed to drain away. Pots were wrapped with plastic to eliminate soil evaporation and then the pot weight was recorded every minute during dry-down on individual balances accurate to two decimal places. Any mass loss was attributed to the transpiration of soil water. Conditions in the chamber were set to VPD of c. 1.4 kPa (temperature of 20.5 ± 1.5°C and relative humidity of 41.7 ± 6.9%). The day of visual wilting of all plants per genotype was recorded and the plants remained under drought there until they died (except *sp12* which didn't die even after several days). Seedlings were considered dead when crispy and dry. The total leaf area of each plant was measured before the experiment by taking photos of all leaves and measuring leaf area using the ImageJ software. Whole-plant transpiration was then normalized by total leaf area.

We also assessed the hydraulic conductances of leaves (K_{leaf}), stems (K_{stem}) and roots (K_{root}) of 20-day-old seedlings ($n = 6$). Seedlings were removed from pots and allowed to fully hydrate inside a glass dome until guttation was observed. An expanded leaf was used to measure K_{leaf} using the evaporative flux method and a hydraulic flowmeter as described earlier (Brodribb & Holbrook, 2006). The K_{stem} was obtained gravimetrically (Sperry et al., 1988) using entire stem segments (which averaged 6.5 ± 1.5 cm for all genotypes) that were cut under the water. Stems were then attached to a water reservoir containing ultrapure water (type 1) (Millipore Synergy Ultrapure Water Purification System; Millipore) that was placed at different heights (0.2, 0.4, 0.6, 0.8 and 1.0 m) and had the water flow passing through them (mL s^{-1}) measured by a glass micropipette connected to the stem tip. The K_{stem} was estimated as the slope of the flow rate versus the water pressure applied. The K_{root} was measured using an adapted pressure chamber method (Miyamoto et al., 2001; Sperry et al., 1988). The roots were immersed in a 50 mL Falcon tube containing ultrapure water (type 1), placed inside a Scholander pressure chamber and connected to a water-filled silicone tube coupled to a precision digital balance (AY 220 model; Shimadzu). Increasing pressures were applied to the chamber (0.01, 0.02, 0.03, 0.04 and 0.05 MPa) and the flow generated (g s^{-1}) was recorded every 30 s for 150 s. The K_{root} was derived from the slope of the flow rate line versus the water pressure applied.

For leaves, the hydraulic conductance was normalized by leaf area. For stems and roots, the hydraulic conductances were not normalized by stem xylem area or by area or mass of roots. Rather they were simply calculated as the ratio of water flows through the sample to the water potential gradient across the sample (Da-li et al., 2022). By doing so, we assess the hydraulic conductance of the whole organ, taking into account both the inherent hydraulic conductivity of the tissue and differences in organ/tissue size (root surface area, stem length and xylem area), which ultimately define the total water flux from roots and stems to the leaves.

2.7 | Statistical analysis

One-way and two-way (data related to the drought experiment) analysis of variance (ANOVA) was applied in all parameters to test whether the treatments show some difference. When we observed significant effects in ANOVA, multiple mean comparisons were performed using Tukey's post hoc test. All statistical tests and graphics were performed using RStudio (v.4.3.0; Posit Team, 2023).

3 | RESULTS

3.1 | ABA levels

The differences in the ability to accumulate ABA across the four genotypes were confirmed by assessing leaf ABA levels (Table 1). The *sit* (416 ng g^{-1} DW) and *not* (962 ng g^{-1} DW) ABA levels were on average one-fourth and half of the WT levels (1726 ng g^{-1} DW). The *sp12* mean level of ABA (3684 ng g^{-1} DW) was over twice that of the WT.

3.2 | Embolism resistance of stems and leaves

When stems of young plants (up to 60-day-old) were subjected to dry-down, xylem resistance to embolism was found to be similar across plants of all four genotypes (Table 2; Figure 1), regardless of their ability to accumulate ABA. For all genotypes, embolism initiated (P_{12}) at approximately −1.00 MPa, reached P_{50} between −1.30 and −1.45 MPa, and reached 88% of xylem embolism (P_{88}) between −1.50 and −1.75 MPa (Table 2). The higher variation in xylem resistance within the genotype was observed for WT and *sp12* plants than for the two ABA-mutants, *sit* and *not* (Figure 1).

TABLE 1 Leaf area, maximum net CO_2 assimilation rate (A), maximum stomatal conductance to water vapour (g_s), maximum transpiration rate (E), intrinsic water-use efficiency (WUE_i), leaf water potential at turgor loss point (Ψ_{TLP}) and minimum leaf conductance (g_{min}) of four tomato genotypes differing in their ability to accumulate foliar ABA: *sitiens (sit)* and *notabilis (not)* are ABA biosynthetic mutants, WT is wild type cv. Ailsa Craig and *sp12* is a transgenic line overaccumulating ABA.

Trait	*n*	*sit*	*not*	WT	*sp12*
Foliar ABA (ng g^{-1} DW)	6	416 ± 26^{c}	962 ± 167^{bc}	1726 ± 131^{b}	3684 ± 634^{a}
Plant leaf area (m^2)	4	0.15 ± 0.03^{b}	0.20 ± 0.01^{a}	0.23 ± 0.01^{a}	0.23 ± 0.03^{a}
A (μmol CO_2 m^{-2} s^{-1})	8	17.63 ± 1.36^{a}	18.58 ± 0.93^{a}	17.77 ± 1.29^{a}	16.21 ± 1.58^{a}
g_s (mol H_2O m^{-2} s^{-1})	8	1.76 ± 0.15^{a}	1.01 ± 0.04^{b}	0.57 ± 0.12^{c}	0.35 ± 0.06^{d}
E (mmol H_2O m^{-2} s^{-1})	8	17.39 ± 0.52^{a}	14.43 ± 0.42^{ab}	10.95 ± 1.48^{b}	6.98 ± 0.91^{c}
WUE_i (A/g_s)	8	10.20 ± 0.61^{c}	18.54 ± 0.83^{bc}	40.31 ± 8.57^{ab}	54.97 ± 7.94^{a}
Ψ_{TLP} (MPa)	6	−0.99 ± 0.08^{ab}	−1.04 ± 0.01^{b}	−0.84 ± 0.02^{a}	−0.99 ± 0.01^{ab}
g_{min} (mmol H_2O m^{-2} s^{-1})	12	28.10 ± 2.06^{a}	20.70 ± 1.68^{b}	6.66 ± 0.95^{c}	4.24 ± 0.48^{c}

Note: Data are mean ± standard error (n is described for each trait). Superscript letters denote results from statistical tests (Tukey, $p < 0.05$) conducted between genotypes.

Abbreviations: ABA, abscisic acid; DW, dry matter.

TABLE 2 Water potential inducing 12% (P_{12}), 50% (P_{50}) and 88% (P_{88}) embolism (optical vulnerability) of leaves and stems or declines in hydraulic conductance of leaves (rehydration kinetics method) of four tomato genotypes differing in their ability to accumulate foliar ABA: *sitiens (sit)* and *notabilis (not)* are ABA biosynthetic mutants, WT is wild type cv. Ailsa Craig and *sp12* is a transgenic line overaccumulating ABA.

Trait	*sit*	*not*	WT	*sp12*
Leaf optical vulnerability (MPa)				
P_{12}	−1.04 ± 0.07^{a}	−1.09 ± 0.09^{a}	−1.04 ± 0.06^{a}	−1.01 ± 0.05^{a}
P_{50}	−1.27 ± 0.03^{a}	−1.38 ± 0.03^{ab}	−1.38 ± 0.06^{ab}	−1.51 ± 0.03^{b}
P_{88}	−1.40 ± 0.06^{a}	−1.50 ± 0.04^{ab}	−1.74 ± 0.12^{b}	−1.63 ± 0.07^{ab}
Stem optical vulnerability (MPa)				
P_{12}	−1.04 ± 0.07^{a}	−1.04 ± 0.03^{a}	−1.10 ± 0.08^{a}	−0.93 ± 0.10^{a}
P_{50}	−1.35 ± 0.07^{a}	−1.33 ± 0.03^{a}	−1.47 ± 0.08^{a}	−1.33 ± 0.09^{a}
P_{88}	−1.48 ± 0.08^{a}	−1.48 ± 0.03^{a}	−1.75 ± 0.15^{a}	−1.69 ± 0.13^{a}
Rehydration kinetics method (MPa)				
P_{12}	−1.21 ± 0.10^{a}	−1.21 ± 0.06^{a}	−1.27 ± 0.06^{a}	−1.29 ± 0.11^{a}
P_{50}	−1.30 ± 0.03^{a}	−1.33 ± 0.03^{ab}	−1.42 ± 0.06^{ab}	−1.48 ± 0.05^{b}
P_{88}	−1.50 ± 0.04^{a}	−1.45 ± 0.05^{a}	−1.50 ± 0.06^{a}	−1.66 ± 0.06^{a}

Note: Data are mean ± standard error ($n = 6$). Superscript letters denote results from statistical tests (Tukey, $p < 0.05$) conducted between genotypes.
Abbreviation: ABA, abscisic acid.

The leaf P_{12} and P_{88} were similar across genotypes as observed by the optical and hydraulic methods (Table 2, and Figures 2 and 3). Differences were observed for the mean P_{50} values of leaves. Similar P_{50} was observed for *not*, the least severe ABA-deficient mutant, WT and the ABA-overaccumulating line *sp12*. The most severe ABA deficient mutant, *sit*, exhibited leaves with xylem that was significantly less resistant to embolism than *sp12*, as observed by the optical (a difference of −0.24 MPa, $p = 0.03$) and the hydraulic method (a difference of −0.18 MPa, $p = 0.04$). In all genotypes, the embolism in the leaf xylem started in the midrib and quickly spread to the higher vein orders (Figure 2; Supporting Information: Table 2). The hydraulic safety margin (HSM), calculated as the difference between the water potential at the turgor loss point (Ψ_{TLP}) and P_{50} in leaves also differed across genotypes, with the two ABA-deficient mutants exhibiting lower HSM (0.37 MPa for *sit* and 0.34 for *not*) than WT (0.54 MPa) and *sp12* (0.52 MPa) (Figure 2). The higher HSM observed for WT plants over the ABA-deficient mutants resulted from its higher Ψ_{TLP} (Table 1).

Overall, changes in Ψ_{TLP} across genotypes were not consistent with the constitutive levels of foliar ABA (Table 1). *Sit*, WT and *sp12* had similar Ψ_{TLP} as well as *sit*, *not* and *sp12*. The only difference in Ψ_{TLP} occurred between *not* (−1.04 MPa) and WT (−0.84 MPa).

3.3 | Maximum and minimum stomatal conductances

Given the contrasting constitutive levels of ABA biosynthesis across the four genotypes, differences in the leaf gas exchange rate between these plants were observed under well-watered conditions (Table 1). Maximum g_s was dependent on the constitutive levels of foliar ABA, such that *sit* mutant plants achieved the highest g_s (1.76 mol m^{-2} s^{-1}), followed by plants of *not* (1.01 mol m^{-2} s^{-1}), WT (0.57 mol m^{-2} s^{-1}) and finally *sp12* (0.35 mol m^{-2} s^{-1}). Changes in g_s translated into changes in *E*, but we observed no differences in *A* across genotypes. Consequently, the WUE_i (calculated as A/g_s) was highest in *sp12* (c. 55) and significantly higher than that of the two ABA-deficient mutant lines (10.20 in *sit* and c. 19 in *not*). Substantial changes in g_{min} were also observed across genotypes, with plants of WT and *sp12* exhibiting the lowest values of g_{min} (6.6 and 4.2 mmol m^{-2} s^{-1}, respectively), followed by plants of *not* (20.2 mmol m^{-2} s^{-1}), and last by *sit* (28.1 mmol m^{-2} s^{-1}). The g_{min} of *not* and *sit* mutant plants were approximately five and seven times that of *sp12* mutant plants, respectively.

Changes in maximum g_s and g_{min} due to genotype differences in ABA biosynthesis were not only caused by a change in stomatal aperture but also by changes in stomatal anatomy (Supporting Information: Figure S1). The *sit* plants exhibited higher stomatal density on both leaf surfaces when compared to WT plants. Besides having more stomata per leaf area, the stomata of *sit* mutant plants were also larger than that of the other genotypes. On the other extreme, *sp12* mutant plants exhibited lower stomatal densities than plants of the other genotypes.

3.4 | Dry-down experiments and time to reach critical water potential

Following water withholding, mature (60-day-old) plants of all genotypes decreased Ψ_{leaf} and g_s (Figure 4). Plants were allowed to

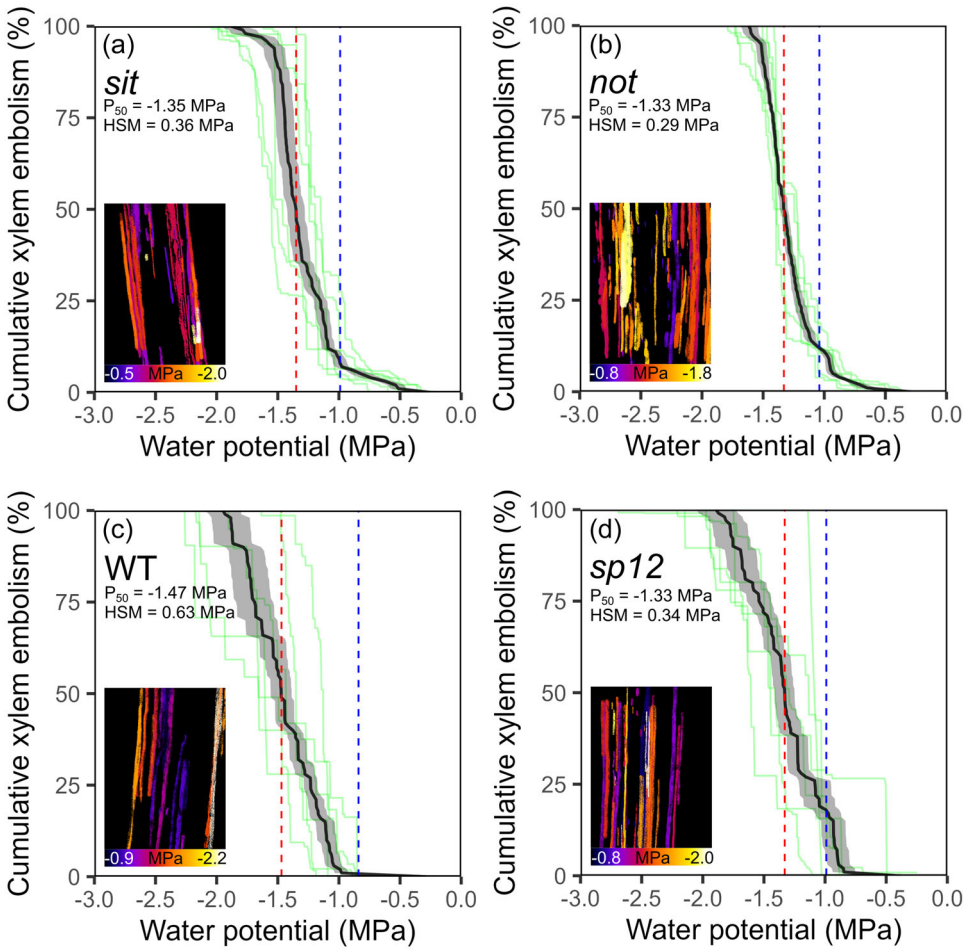


FIGURE 1 Stem xylem vulnerability curves obtained from the optical vulnerability technique of four tomato genotypes differing in their ability to accumulate foliar ABA: *sitiens (sit)* (a) and *notabilis (not)* (b) are ABA biosynthetic mutants, WT is wild type cv. Ailsa Craig (c) and *sp12* is a transgenic line overaccumulating ABA (d). Black line and shadow represent means and standard errors ($n = 6$), respectively. Green lines are replicates. Blue dashed lines represent leaf turgor loss points and red dashed lines indicate the water potentials associated with 50% of cumulative stem xylem embolism (P_{50}). The difference between these two parameters is the hydraulic safety margin (HSM). ABA, abscisic acid.

dry until the critical Ψ_{leaf} of c. −1.30 MPa, which was selected because of close proximity with the mean stem P_{50} of plants of *sit*, *not* and WT. The time for plants to reach this critical threshold was substantially different across genotypes: 5, 6, 9 and 12 days for *not*, *sit*, WT and *sp12* plants, respectively (Figure 4a). Note that the total leaf area per plant was similar across droughted plants from all genotypes (Figure 4d). Plants of WT and *sp12* had tightly closed stomata by the time plants reached the critical Ψ_{leaf}, while *sit* and *not* mutant plants continued to exhibit relatively high g_s (Figure 4b). Plants from all genotypes showed visible wilting at the critical Ψ_{leaf}, and the leaf water turgor could recover after rewatering (Supporting Information: Figure S2). They also displayed limited recovery in K_{leaf} even after 2 days of rewatering (Figure 4c), indicating that an embolism in the leaf xylem had occurred. Decreases in K_{leaf} were 58%, 51%, 50% and 41% for plants of *sit*, *not*, WT and *sp12*, respectively.

The dry-down experiment with seedlings demonstrated that plants of the two ABA-deficient mutants wilted and died before the WT (Figure 5). The *sit* seedlings were the first to wilt (at Day 5), despite having the lowest total leaf area. Plants of *not*, WT and *sp12* wilted at Days 11, 14 and 16 after water withholding. Plants of *sp12* were the only ones alive after 18 days without irrigation. Seedlings of *not*, WT and *sp12* had similar K_{leaf}, K_{stem} and K_{root}. The *sit* plants exhibited lower K_{stem} than *not* and lower K_{root} than WT plants.

4 | DISCUSSION

Our findings demonstrate that the embolism resistances of stems and leaves are essentially similar across young plants of tomato with different abilities to accumulate ABA. In contrast to the minor effect of ABA levels on the xylem physiology, our findings reinforce the critical role of ABA in reducing maximum g_s and demonstrate for the first time its effect on lowering g_{min}, thus improving WUE during well-watered conditions and delaying plant dehydration and damage during drought.

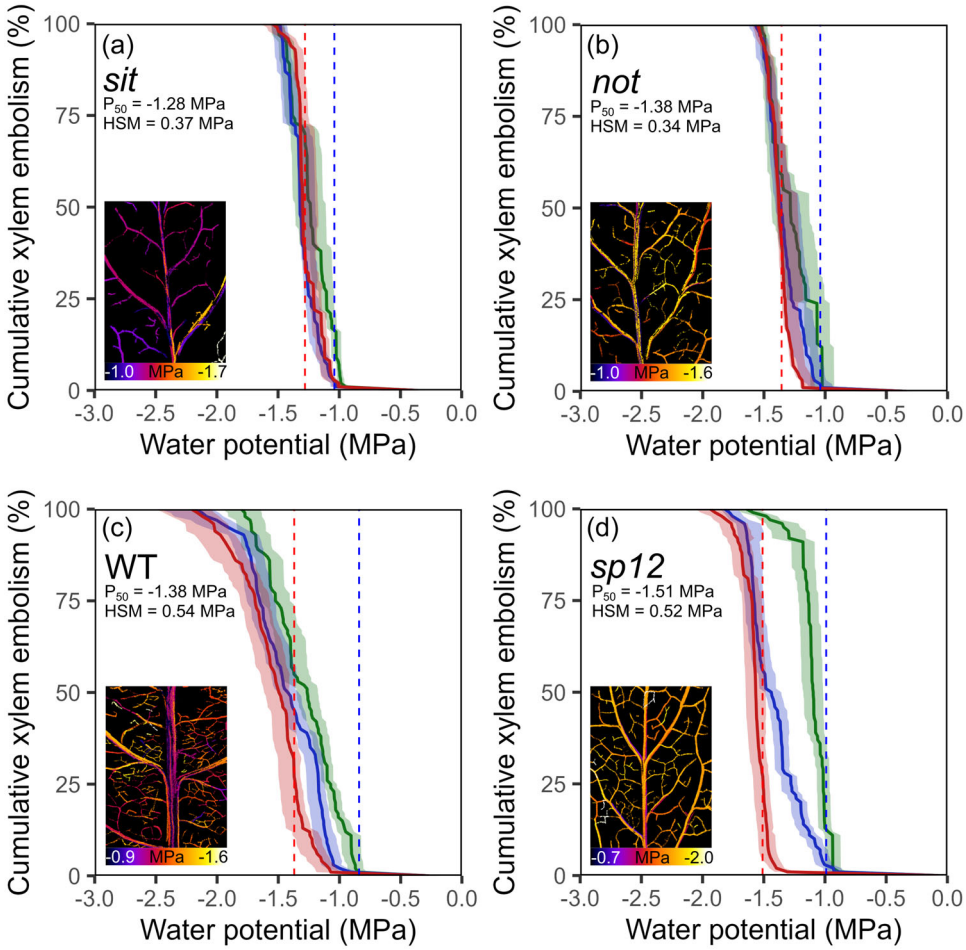


FIGURE 2 Optical vulnerability curves obtained from leaves of four tomato genotypes differing in their ability to accumulate foliar ABA: *sitiens (sit)* (a) and *notabilis (not)* (b) are ABA biosynthetic mutants, WT is wild type cv. Ailsa Craig (c) and *sp12* is a transgenic line overaccumulating ABA (d). Midrib is represented by green lines, secondary veins by blue lines, and minor veins by red lines. Data are mean (highlighted lines) ± standard error (shadow) ($n = 6$). Blue dashed lines represent leaf turgor loss points and red dashed lines indicate the water potentials associated with 50% of cumulative xylem embolism for the whole leaf (P_{50}). The difference between these two parameters is the hydraulic safety margin (HSM). ABA, abscisic acid. [Color figure can be viewed at wileyonlinelibrary.com]

4.1 | ABA levels and xylem embolism resistance

Our results show that the internal levels of ABA do not impact the embolism resistance of stems of young (60 days old) plants of tomato in a similar way to what was observed for very old (170 day old) plants (Lamarque et al., 2020). This result contrasts with the negative impact of increased ABA levels on the stem embolism resistance of tomato plants at 90 and 120 days old (Lamarque et al., 2020). Therefore, the decreases in embolism resistance in overaccumulating ABA plants appear to only occur during part of the plant life cycle, which might be associated with differences in stem anatomy throughout the plant development.

In our study, the 60-day-old plants from all four genotypes were at a similar stage of secondary growth (Supporting Information: Figure S3). At this age, stems from all genotypes had started transitioning from primary to secondary growth, and they showed similar areas of secondary xylem. In the case of Lamarque et al. (2020), images of stems of 120-day-old plants of *sp12* and WT obtained by microcomputed tomography show that the WT plants exhibited much more developed secondary xylem than the *sp12* plants at the time that the experiment was conducted, which might have been caused by the increased constitutive levels of ABA. Stems of older plants of tomato have long been known to exhibit secondary growth, with a higher proportion of secondary xylem (often named wood), and a higher degree of lignification than younger plants (Thompson & Heimsch, 1964). Such an increased degree of woodiness and lignification has previously been associated with increased xylem resistance to embolism in stems of herbaceous plants that can develop secondary xylem (Dória et al., 2019; Thonglim et al., 2021, 2023). In very old (170 days old) tomato plants of WT and *sp12*, in which similar stem xylem resistances were observed (Lamarque et al., 2020), a complete transition to secondary growth is likely to have occurred.

A number of studies demonstrate that increased ABA levels associate with vascular cambium dormancy in woody species (Fromm, 1997; Mwange et al., 2005; Hou et al., 2006; Ding et al., 2016), thus supporting our hypothesis of delayed secondary xylem

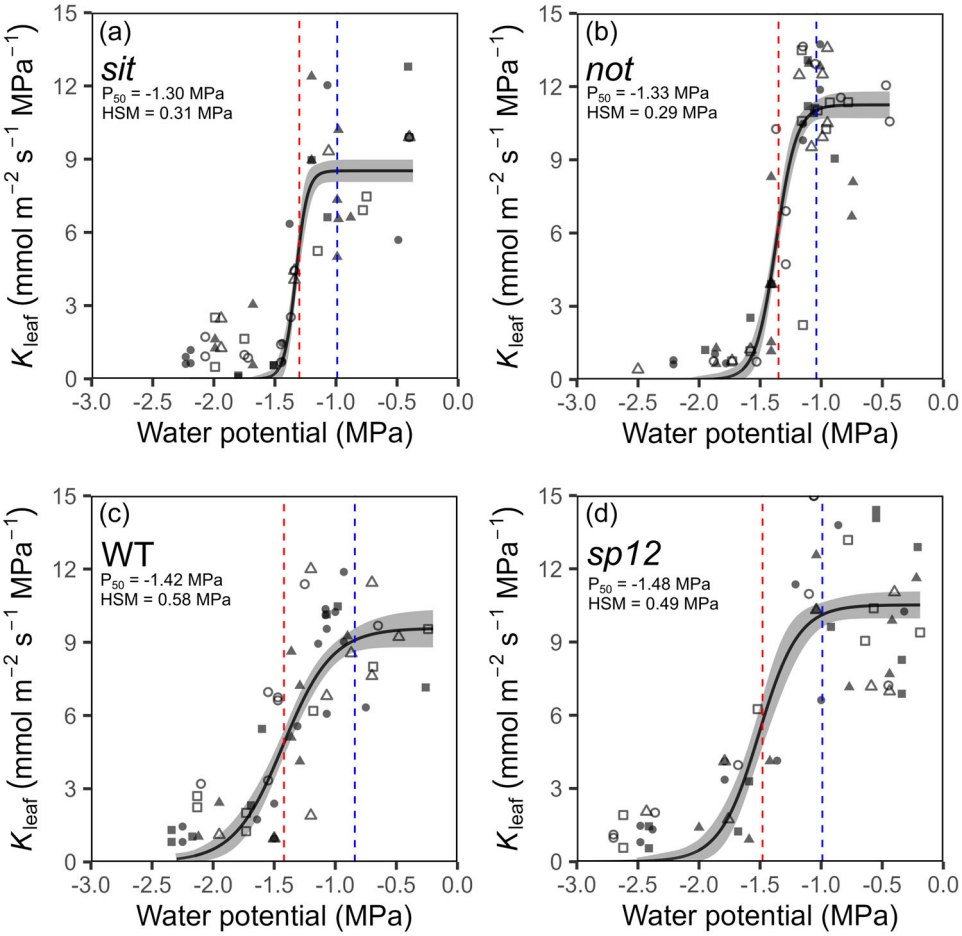


FIGURE 3 Decline in leaf hydraulic conductance (K_{leaf}) during leaf dehydration for four tomato genotypes differing in their ability to accumulate foliar ABA: *sitiens (sit)* (a) and *notabilis (not)* (b) are ABA biosynthetic mutants, WT is wild type cv. Ailsa Craig (c) and *sp12* is a transgenic line overaccumulating ABA (d). Black continuous lines are the predicted values from the three-parameter sigmoidal equation performed using all data and shadows represent standard errors. Different symbols indicate individual plants ($n = 6$). Blue dashed lines represent leaf turgor loss points and red dashed lines indicate the water potentials associated with 50% loss in K_{leaf} (P_{50}). The difference between these two parameters is the hydraulic safety margin (HSM). ABA, abscisic acid. [Color figure can be viewed at wileyonlinelibrary.com]

development in plants of *sp12* over the WT. In any case, further experiments thoroughly assessing the transition from primary to secondary growth of ABA mutants and over-accumulating ABA lines are necessary to confirm whether ABA delays the formation of secondary xylem in herbaceous plants.

Increased ABA biosynthesis was also essentially disconnected from leaf embolism resistance. A marginal increase (0.24 MPa) in P_{50} was only observed when comparing genotypes with the extremes of ABA level (*sp12* vs. *sit* mutant plants). The same increase was not observed for P_{12} and P_{88}. This result is not surprising given the absence of secondary xylem development in leaves.

4.2 | ABA reduces water loss and delays plant dehydration

The overaccumulation of ABA resulted in partially closed stomata, and thus in lower water loss from leaves to the atmosphere. Given that photosynthesis was not affected, *sp12* mutant plants operated at elevated WUE, as previously reported by Thompson, Andrews et al. (2007) through gas exchange, gravimetric and carbon isotope discrimination methods. The overaccumulation of ABA also resulted in very low minimum leaf conductance likely due to lower stomatal density and size (Machado et al., 2021; Muchow & Sinclair, 1989). Declines in stomatal density have been previously associated with higher ABA levels—likely due to increased cell turgor and growth (Tanaka et al., 2013; Xie et al., 2006)—and here we demonstrate that increased ABA levels are also associated with lower minimum leaf conductance. Low minimum leaf conductance is of paramount importance for plants to minimize residual transpiration after stomatal closure and delay further dehydration below thresholds of hydraulic and photosynthetic damage (Duursma et al., 2019; Gleason et al., 2014).

Due to changes in maximum and minimum stomatal conductances, genotypes with contrasting ABA levels reached the same critical water potential after very different times. This demonstrates

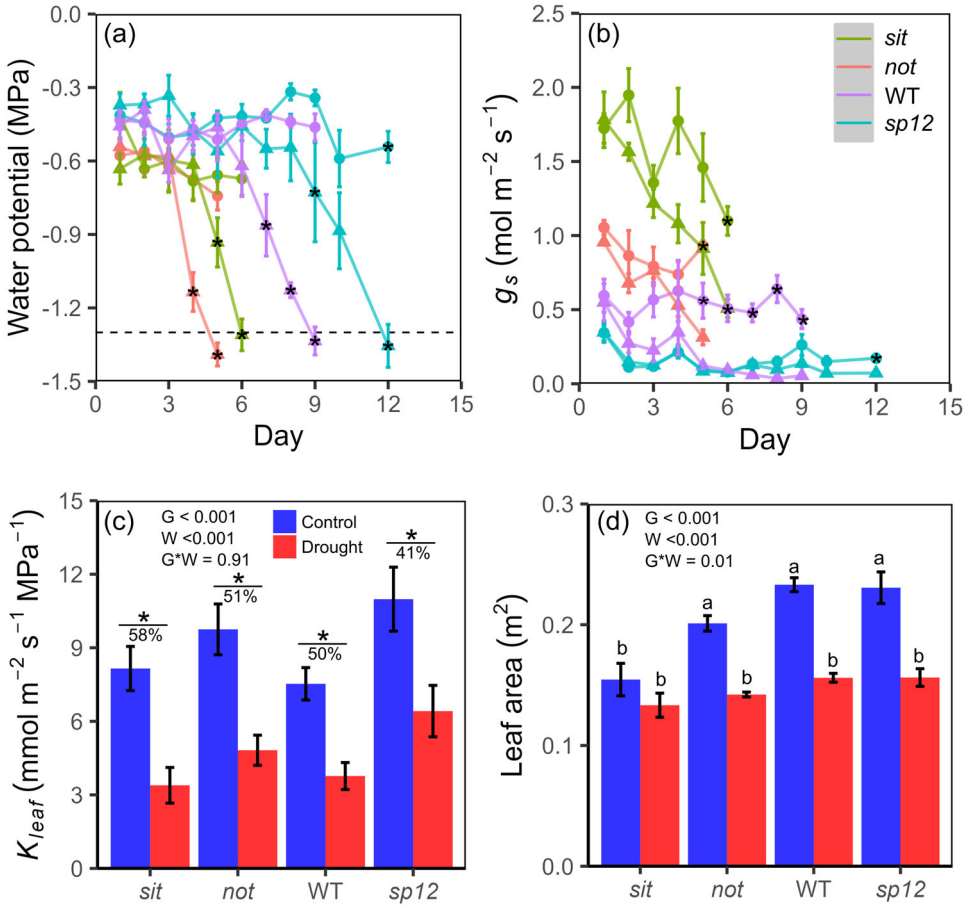


FIGURE 4 (a) Midday leaf water potential and (b) stomatal conductance (g_s) throughout a dry-down experiment of four tomato genotypes differing in their ability to accumulate foliar ABA: *sitiens* (*sit*) and *notabilis* (*not*) are ABA biosynthetic mutants, WT is wild type cv. Ailsa Craig and *sp12* is a transgenic line overaccumulating ABA. Plants had water withheld after the first measurement and they were maintained under drought until the critical water potential of −1.30 MPa (black dashed line in a). Circles represent control plants and triangles, droughted plants. (c) Leaf hydraulic conductance (K_{leaf}) of control and droughted plants 2 days after irrigation was restored. (d) Plant leaf area at the end of the experiment. Data are mean ± standard error ($n = 4$). The two-way ANOVA results are shown. Asterisks denote statistical differences (Tukey, $p < 0.05$) for watering conditions (control vs. drought) and letters allow comparison between treatments. See Supporting Information: Figure S1 for representative images of plants during this experiment. ABA, abscisic acid; ANOVA, analysis of variance; G, genotype; W, watering condition. [Color figure can be viewed at wileyonlinelibrary.com]

that not only the water potential inducing embolism and damage is important but also the time needed by plants to reach those threshold water potentials (Blackman et al., 2019). Another important component influencing dehydration time is the total leaf area per plant and the leaf distribution across the plant (plant architecture), both influencing the total water loss (Blackman et al., 2019). At the same time, the hydraulic conductances of leaves, stems and roots limit the water supply to the leaves, thus buffering water loss to the atmosphere and plant dehydration.

For the dry-down of adult plants, the higher leaf area in *not* compared to *sit* mutant plants might explain why *not* mutant plants reached the critical water potential of −1.30 MPa before *sit* mutant plants, despite lower minimum rates of conductance in *not* over *sit* plants. Besides, adult plants of the *sit* mutant exhibited curled leaves and shorter internodes (Table 1) (Stubbe, 1957, 1958), and such modifications in plant architecture might have also contributed to a delayed dehydration in this genotype. For the dry-down of seedlings, *sit* plants reached turgor loss point before *not* plants, despite the lower total leaf area. This might have been driven by its substantially higher evaporation rate per unit area, as well as by a potentially lower water flux from roots and stems to the leaves (Figure 5). ABA-deficient mutants are known to have low K_{root} (Tal & Nevo, 1973), and the combination of low K_{root} and inability to close stomata would inevitably lead to rapid wilting in drying soil or high VPD. In other studies, *sp12* was reported to have higher K_{root} than WT, consistent with a positive relationship between ABA level and K_{root} (Thompson, Andrews, et al., 2007). In the case of *not*, *WT* and *sp12* plants, changes in time were found despite similar total leaf areas and hydraulic conductances, likely due to changes in maximum and minimum stomatal conductances.

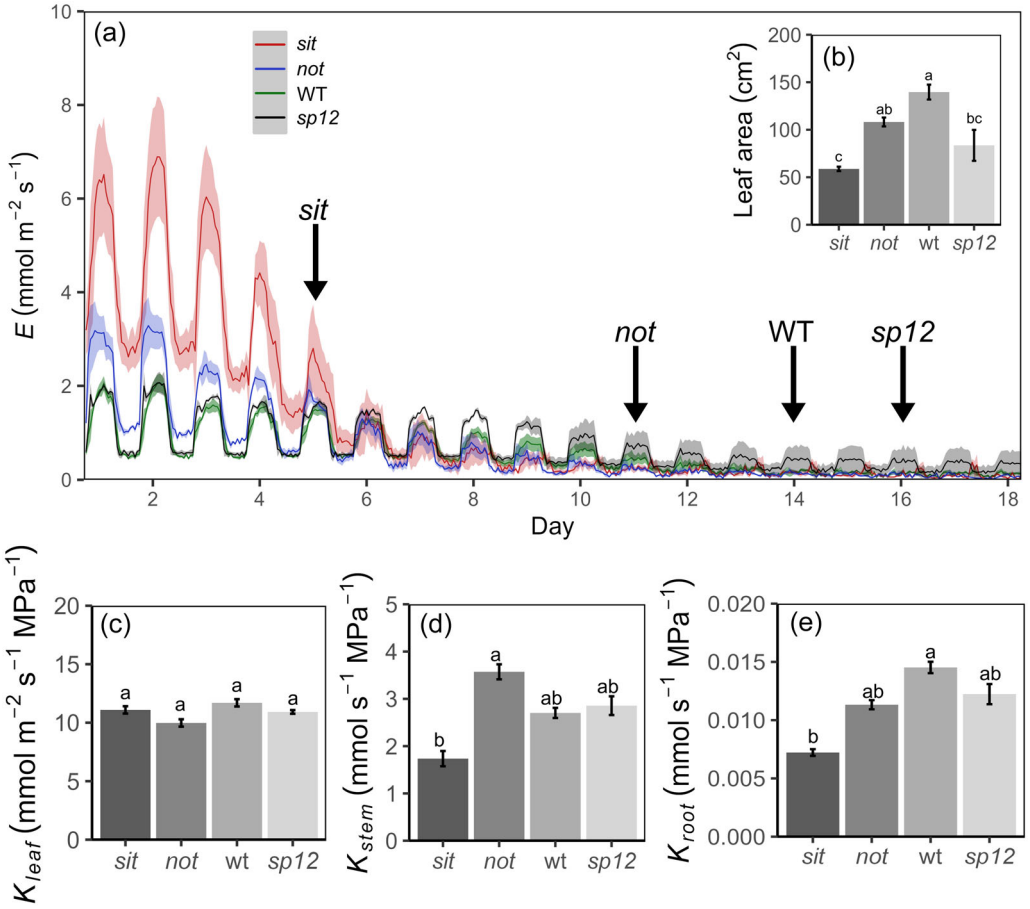


FIGURE 5 Dry-down experiment using seedlings of four tomato genotypes differing in their ability to accumulate foliar ABA: *sitiens (sit)* and *notabilis (not)* are ABA biosynthetic mutants, WT is wild type cv. Ailsa Craig and *sp12* is a transgenic line overaccumulating ABA. (a) Whole-plant transpiration rate throughout the drought days. Black arrows indicate the day at which plants from the four genotypes wilted. (b) Total leaf area per plant. (c) Leaf hydraulic conductance (K_{leaf}) normalized by leaf area. (d) Stem hydraulic conductance (K_{stem}). (e) Root hydraulic conductance (K_{root}). Shadows and error bars represent standard error ($n = 4$). Letters over the error bars denote results from statistical tests (Tukey, $p < 0.05$) conducted between genotypes. ABA, abscisic acid.

5 | CONCLUSION

The impact of ABA on drought resistance in young plants of tomato is essentially associated with stomatal function, and not with xylem resistance to embolism. Leaves and stems of genotypes spanning a large variation in the constitutive levels of ABA have essentially similar embolism resistance, which does not seem to occur throughout the plant life cycle (Lamarque et al., 2020). Genotypes with higher constitutive levels of ABA have lower maximum stomatal and minimum leaf conductances, efficiently improving WUE under well-watered conditions and delaying hydraulic dysfunction and damage during drought. Given that tomato plants are often cultivated with supplemental irrigation, improvements in water conservation resulting from increased amounts of ABA are likely more important for agriculture than the potential declines in embolism resistance during part of the plant life cycle. We still lack, however, studies assessing the impact of ABA on plant productivity, such that genotypes overaccumulating ABA can finally be used in agriculture.

ACKNOWLEDGEMENTS

The authors acknowledge the use of Bindley Bioscience Center at Purdue University (National Institutes of Health-funded Indiana Clinical and Translational Sciences Institute), particularly the Metabolite Profiling Facility. This study was supported by the USDA National Institute of Food and Agriculture, Hatch Project 7003279 (Amanda A. Cardoso) and the National Science Foundation Grant IOS-2140119 (Scott A. M. McAdam).

DATA AVAILABILITY STATEMENT

The data that support the findings of this study are available from the corresponding author upon reasonable request.

ORCID

Leonardo A. Oliveira http://orcid.org/0000-0003-3048-2963
Scott A. M. McAdam http://orcid.org/0000-0002-9625-6750
Amanda A. Cardoso http://orcid.org/0000-0001-7078-6246

REFERENCES

Avila, R.T., Kane, C.N., Batz, T.A., Trabi, C., Damatta, F.M., Jansen, S. et al. (2023) The relative area of vessels in xylem correlates with stem embolism resistance within and between genera. *Tree Physiology*, 43, 75–87.

Blackman, C.J. & Brodribb, T.J. (2011) Two measures of leaf capacitance: insights into the water transport pathway and hydraulic conductance in leaves. *Functional Plant Biology*, 38, 118.

Blackman, C.J., Brodribb, T.J. & Jordan, G.J. (2010) Leaf hydraulic vulnerability is related to conduit dimensions and drought resistance across a diverse range of woody angiosperms. *New Phytologist*, 188, 1113–1123.

Blackman, C.J., Li, X., Choat, B., Rymer, P.D., de Kauwe, M.G., Duursma, R.A. et al. (2019) Desiccation time during drought is highly predictable across species of *Eucalyptus* from contrasting climates. *New Phytologist*, 224, 632–643.

Brodribb, T.J., Bienaimé, D. & Marmottant, P. (2016) Revealing catastrophic failure of leaf networks under stress. *Proceedings of the National Academy of Sciences of the United States of America*, 113, 4865–4869.

Brodribb, T.J. & Cochard, H. (2009) Hydraulic failure defines the recovery and point of death in water-stressed conifers. *Plant Physiology*, 149, 575–584.

Brodribb, T.J. & Holbrook, N.M. (2006) Declining hydraulic efficiency as transpiring leaves desiccate: two types of response. *Plant, Cell and Environment*, 29, 2205–2215.

Burbidge, A., Grieve, T.M., Jackson, A., Thompson, a, McCarty, D.R. & Taylor, I.B. (1999) Characterization of the ABA-deficient tomato mutant *notabilis* and its relationship with maize *Vp14*. *The Plant Journal*, 17, 427–431.

Cardoso, A.A., Batz, T.A. & McAdam, S.A.M. (2020) Xylem embolism resistance determines leaf mortality during drought in *Persea americana*. *Plant Physiology*, 182, 547–554.

Cardoso, A.A., Brodribb, T.J., Lucani, C.J., DaMatta, F.M. & McAdam, S.A.M. (2018) Coordinated plasticity maintains hydraulic safety in sunflower leaves. *Plant, Cell & Environment*, 41, 2567–2576.

Cardoso, A.A., Kane, C.N., Rimer, I.M. & McAdam, S.A.M. (2022) Seeing is believing: what visualising bubbles in the xylem has revealed about plant hydraulic function. *Functional Plant Biology*, 49, 759–772.

Choat, B., Jansen, S., Brodribb, T.J., Cochard, H., Delzon, S., Bhaskar, R. et al. (2012) Global convergence in the vulnerability of forests to drought. *Nature*, 491, 752–755.

Creek, D., Lamarque, L.J., Torres-Ruiz, J.M., Parise, C., Burlett, R., Tissue, D.T. et al. (2020) Xylem embolism in leaves does not occur with open stomata: evidence from direct observations using the optical visualization technique. *Journal of Experimental Botany*, 71, 1151–1159.

Creelman, R.A. & Zeevaart, J.A.D. (1985) Abscisic acid accumulation in spinach leaf slices in the presence of penetrating and nonpenetrating solutes. *Plant Physiology*, 77, 25–28.

Dai, A. (2013) Increasing drought under global warming in observations and models. *Nature Climate Change*, 3, 52–58.

Da-li, G., Lei, L., Yu-sen, Y., Feng-wang, M. & Qing-mei, G. (2022) Factors affecting hydraulic conductivity and methods to measure in plants. *Journal of Integrative Agriculture*, 21, 310–315.

Daszkowska-Golec, A. & Szarejko, I. (2013) Open or close the gate - stomata action under the control of phytohormones in drought stress conditions. *Frontiers in Plant Science*, 4, 1–16.

Ding, Q., Zeng, J., & He, X.Q. (2016) MiR169 and its target PagHAP2-6 regulated by ABA are involved in poplar cambium dormancy. *Journal of Plant Physiology*, 198, 1–9.

Dixon, H.H. & Joly, J. (1895) XII. On the ascent of sap. *Philosophical Transactions of the Royal Society B*, 186, 563–576.

Dória, L.C., Meijs, C., Podadera, D.S., del Arco, M., Smets, E., Delzon, S. et al. (2019) Embolism resistance in stems of herbaceous Brassicaceae and Asteraceae is linked to differences in woodiness and precipitation. *Annals of Botany*, 124, 1–14.

Dória, L.C., Podadera, D.S., Arco, M., Chauvin, T., Smets, E., Delzon, S. et al. (2018) Insular woody daisies (*Argyranthemum*, Asteraceae) are more resistant to drought-induced hydraulic failure than their herbaceous relatives. *Functional Ecology*, 32, 1467–1478.

Duursma, R.A., Blackman, C.J., Lopéz, R., Martin-StPaul, N.K., Cochard, H. & Medlyn, B.E. (2019) On the minimum leaf conductance: its role in models of plant water use, and ecological and environmental controls. *New Phytologist*, 221, 693–705.

Fromm J. (1997) Hormonal physiology of wood growth in willow (Salix viminalis L.): Effects of spermine and abscisic acid. *Wood Science and Technology*, 31, 119–130.

Gleason, S.M., Blackman, C.J., Cook, A.M., Laws, C.A. & Westoby, M. (2014) Whole-plant capacitance, embolism resistance and slow transpiration rates all contribute to longer desiccation times in woody angiosperms from arid and wet habitats. *Tree Physiology*, 34, 275–284.

Harrison, E., Burbidge, A., Okyere, J.P., Thompson, A.J. & Taylor, I.B. (2011) Identification of the tomato ABA-deficient mutant *sitiens* as a member of the ABA-aldehyde oxidase gene family using genetic and genomic analysis. *Plant Growth Regulation*, 64, 301–309.

Helander, J.D.M., Vaidya, A.S. & Cutler, S.R. (2016) Chemical manipulation of plant water use. *Bioorganic & Medicinal Chemistry*, 24, 493–500.

Hou, H.-W., Zhou, Y.-T., Mwange, K.-N., Li, W.-F., He, X.-Q., & Cui, K.-M. (2006) ABP1 expression regulated by IAA and ABA is associated with the cambium periodicity in Eucommia ulmoides Oliv. *Journal of Experimental Botany*, 57, 3857–3867.

Isasa, E., Link, R.M., Jansen, S., Tezeh, F.R., Kaack, L., Sarmento Cabral, J. et al. (2023) Addressing controversies in the xylem embolism resistance–vessel diameter relationship. *New Phytologist*, 238, 283–296.

Johnson, K.M., Lucani, C. & Brodribb, T.J. (2022) In vivo monitoring of drought-induced embolism in *Callitris rhomboidea* trees reveals wide variation in branchlet vulnerability and high resistance to tissue death. *New Phytologist*, 233, 207–218.

Lamarque, L.J., Delzon, S., Toups, H., Gravel, A.I., Corso, D., Badel, E. et al. (2020) Over-accumulation of abscisic acid in transgenic tomato plants increases the risk of hydraulic failure. *Plant, Cell & Environment*, 43, 548–562.

Lesk, C., Rowhani, P. & Ramankutty, N. (2016) Influence of extreme weather disasters on global crop production. *Nature*, 529, 84–87.

Lobell, D.B. & Field, C.B. (2007) Global scale climate-crop yield relationships and the impacts of recent warming. *Environmental Research Letters*, 2, 014002.

Loepfe, L., Martinez-Vilalta, J., Piñol, J. & Mencuccini, M. (2007) The relevance of xylem network structure for plant hydraulic efficiency and safety. *Journal of Theoretical Biology*, 247, 788–803.

Machado, R., Loram-Lourenço, L., Farnese, F.S., Alves, R.D.F.B., de Sousa, L.F., Silva, F.G. et al. (2021) Where do leaf water leaks come from? Trade-offs underlying the variability in minimum conductance across tropical savanna species with contrasting growth strategies. *New Phytologist*, 229, 1415–1430.

McAdam, S. (2015) Physicochemical quantification of abscisic acid levels in plant tissues with an added internal standard by ultra-performance liquid chromatography. *Bio-Protocol*, 5, e1599–e1612.

McAdam, S.A.M. & Brodribb, T.J. (2016) Linking turgor with ABA biosynthesis: implications for stomatal responses to vapor pressure deficit across land plants. *Plant Physiology*, 171, 2008–2016.

McAdam, S.A.M. & Brodribb, T.J. (2018) Mesophyll cells are the main site of abscisic acid biosynthesis in water-stressed leaves. *Plant Physiology*, 177, 911–917.

McAdam, S.A.M. & Cardoso, A.A. (2019) The recurrent evolution of extremely resistant xylem. *Annals of Forest Science*, 76, 2.

Mega, R., Abe, F., Kim, J.S., Tsuboi, Y., Tanaka, K., Kobayashi, H. et al. (2019) Tuning water-use efficiency and drought tolerance in wheat using abscisic acid receptors. *Nature Plants*, 5, 153–159.

Miyamoto, N., Steudle, E., Hirasawa, T. & Lafitte, R. (2001) Hydraulic conductivity of rice roots. *Journal of Experimental Botany*, 52, 1835–1846.

Mrad, A., Johnson, D.M., Love, D.M. & Domec, J.C. (2021) The roles of conduit redundancy and connectivity in xylem hydraulic functions. *New Phytologist*, 231, 996–1007.

Muchow, R.C. & Sinclair, T.R. (1989) Epidermal conductance, stomatal density and stomatal size among genotypes of *Sorghum bicolor* (L.) Moench. *Plant, Cell and Environment*, 12, 425–431.

Mwange, K.N.K., Hou, H.W., Wang, Y.Q., He, X.Q., & Cui, K.M. (2005) Opposite patterns in the annual distribution and time-course of endogenous abscisic acid and indole-3-acetic acid in relation to the periodicity of cambial activity in Eucommia ulmoides Oliv. *Journal of Experimental Botany*, 56, 1017–1028.

Pierce, M. & Raschke, K. (1980) Correlation between loss of turgor and accumulation of abscisic acid in detached leaves. *Planta*, 148, 174–182.

Posit Team. (2023). *RStudio: Integrated development environment for R*.

Rodriguez-Dominguez, C.M., Carins Murphy, M.R., Lucani, C. & Brodribb, T.J. (2018) Mapping xylem failure in disparate organs of whole plants reveals extreme resistance in olive roots. *New Phytologist*, 218, 1025–1035.

Scoffoni, C., Albuquerque, C., Brodersen, C.R., Townes, S.V., John, G.P., Bartlett, M.K. et al. (2017) Outside-xylem vulnerability, not xylem embolism, controls leaf hydraulic decline during dehydration. *Plant Physiology*, 173, 1197–1210.

Sperry, J.S., Donnelly, J.R. & Tyree, M.T. (1988) A method for measuring hydraulic conductivity and embolism in xylem. *Plant, Cell and Environment*, 11, 35–40.

Stubbe, H. (1957) Mutanten der Kulturtomate *Lycopersicon esculentum* Miller I. *Die Kulturpflanze*, 5, 190–220.

Stubbe, H. (1958) Mutanten der Kulturtomate *Lycopersicon esculentum* Miller II. *Die Kulturpflanze*, 6, 89–115.

Tal, M. & Nevo, Y. (1973) Abnormal stomatal behavior and root resistance, and hormonal imbalance in three wilty mutants of tomato. *Biochemical Genetics*, 8, 291–300.

Tanaka, Y., Nose, T., Jikumaru, Y. & Kamiya, Y. (2013) ABA inhibits entry into stomatal-lineage development in *Arabidopsis* leaves. *The Plant Journal*, 74, 448–457.

Thompson, A.J., Andrews, J., Mulholland, B.J., McKee, J.M.T., Hilton, H.W., Horridge, J.S. et al. (2007) Overproduction of abscisic acid in tomato increases transpiration efficiency and root hydraulic conductivity and influences leaf expansion. *Plant Physiology*, 143, 1905–1917.

Thompson, N.P. & Heimsch, C. (1964) Stem anatomy and aspects of development in tomato. *American Journal of Botany*, 51, 7–19.

Thompson, A.J., Jackson, A.C., Symonds, R.C., Mulholland, B.J., Dadswell, A.R., Blake, P.S. et al. (2000) Ectopic expression of a tomato 9-cis-epoxycarotenoid dioxygenase gene causes over-production of abscisic acid. *The Plant Journal*, 23, 363–374.

Thompson, A.J., Mulholland, B.J., Jackson, A.C., McKee, J.M.T., Hilton, H.W., Symonds, R.C. et al. (2007) Regulation and manipulation of ABA biosynthesis in roots. *Plant, Cell and Environment*, 30, 67–78.

Thonglim, A., Bortolami, G., Delzon, S., Larter, M., Offringa, R., Keurentjes, J.J.B. et al. (2023) Drought response in *Arabidopsis* displays synergistic coordination between stems and leaves. *Journal of Experimental Botany*, 74, 1004–1021.

Thonglim, A., Delzon, S., Larter, M., Karami, O., Rahimi, A., Offringa, R. et al. (2021) Intervessel pit membrane thickness best explains variation in embolism resistance amongst stems of *Arabidopsis thaliana* accessions. *Annals of Botany*, 128, 171–182.

Trueba, S., Pan, R., Scoffoni, C., John, G.P., Davis, S.D. & Sack, L. (2019) Thresholds for leaf damage due to dehydration: declines of hydraulic function, stomatal conductance and cellular integrity precede those for photochemistry. *New Phytologist*, 223, 134–149.

Tyree, M.T. & Hammel, H.T. (1972) The measurement of the turgor pressure and the water relations of plants by the pressure-bomb technique. *Journal of Experimental Botany*, 23, 267–282.

Tyree, M.T. & Sperry, J.S. (1989) Vulnerability of xylem to cavitation and embolism. *Annual Review of Plant Physiology and Plant Molecular Biology*, 40, 19–36.

Venturas, M.D., Sperry, J.S. & Hacke, U.G. (2017) Plant xylem hydraulics: what we understand, current research, and future challenges. *Journal of Integrative Plant Biology*, 59, 356–389.

Xie, X., Wang, Y., Williamson, L., Holroyd, G.H., Tagliavia, C., Murchie, E. et al. (2006) The identification of genes involved in the stomatal response to reduced atmospheric relative humidity. *Current Biology*, 16, 882–887.

Zhang, F.-P., Sussmilch, F., Nichols, D.S., Cardoso, A.A., Brodribb, T.J. & McAdam, S.A.M. (2018) Leaves, not roots or floral tissue, are the main site of rapid, external pressure-induced ABA biosynthesis in angiosperms. *Journal of Experimental Botany*, 69, 1261–1267.

SUPPORTING INFORMATION

Additional supporting information can be found online in the Supporting Information section at the end of this article.

How to cite this article: Haverroth, E.J., Oliveira, L.A., Andrade, M.T., Taggart, M., McAdam, S.A.M., Zsögön, A. et al. (2023) Abscisic acid acts essentially on stomata, not on the xylem, to improve drought resistance in tomato. *Plant, Cell & Environment*, 46, 3229–3241.
https://doi.org/10.1111/pce.14676



https://dspace.org/

Abscisic acid acts essentially on stomata, not on xylem, to improve drought resistance in tomato

Haverroth, Eduardo J.; Oliveira, Leonardo A.; Andrade, Moab T.; Taggart, Matthew; McAdam, Scott A. M. ...

2023-11-01
Wiley
https://doi.org/10.1111/pce.14676
Haverroth EJ, Oliveira LA, Andrade MT, et al., (2023) Abscisic acid acts essentially on stomata, not on xylem, to improve drought resistance in tomato. Plant, Cell and Environment, Volume 46, Issue 11, November 2023, pp. 3229-3241

Downloaded from a DSpace repository. https://dspace.org/